Electronic band structure of graphene from resonant soft x-ray spectroscopy: The role of core-hole effects

L. Zhang,[1,2] N. Schwertfager,[3,4] T. Cheiwchanchamnangij,[3] X. Lin,[2,5] P.-A. Glans-Suzuki,[2] L. F. J. Piper,[6] S. Limpijumnong,[4] Y. Luo,[5,7] J. F. Zhu,[1,*] W. R. L. Lambrecht,[3,†] and J.-H. Guo[2,‡]

[1]*National Synchrotron Radiation Laboratory, University of Science and Technology of China, Hefei 230029, China*

[2]*Advanced Light Source, Lawrence Berkeley National Laboratory, Berkeley, California 94720, USA*

[3]*Department of Physics, Case Western Reserve University, Cleveland, Ohio 44106-7079, USA*

[4]*School of Physics, Suranaree University of Technology, Nakhon Ratchasima 30000, Thailand*

[5]*Division of Theoretical Chemistry and Biology, School of Biotechnology, Royal Institute of Technology, S-106 91 Stockholm, Sweden*

[6]*Department of Physics, Applied Physics and Astronomy, Binghamton University, Binghamton, New York 13902, USA*

[7]*Hefei National Laboratory for Physical Science at the Microscale, University of Science and Technology of China, Hefei 230029, China*

(Received 24 July 2012; revised manuscript received 7 November 2012; published 26 December 2012)

The electronic structure and band dispersion of graphene on SiO_2 have been studied by x-ray-absorption spectroscopy (XAS), x-ray-emission spectroscopy (XES), and resonant inelastic x-ray scattering (RIXS). Using first-principles calculations, it is found that the core-hole effect is dramatic in XAS while it has negligible consequences in XES. Strong dispersive features, due to the conservation of crystal momentum, are observed in RIXS spectra. Simulated RIXS spectra based on the Kramers-Heisenberg theory agree well with the experimental results, provided a shift between RIXS and XAS due to the absence or presence of the core hole is taken into account.

DOI: 10.1103/PhysRevB.86.245430 PACS number(s): 73.22.Pr, 71.10.Li, 78.70.Dm, 78.70.En

I. INTRODUCTION

The recent discovery of graphene has attracted intense research interest due to its extraordinary properties, such as high carrier mobility,[1] strong mechanical strength,[2] and tunable band gap.[3] There are several methods to prepare graphene samples, for example, micromechanical cleavage of graphite,[1] annealing of an SiC single crystal at high temperature,[4] and chemical vapor deposition (CVD) epitaxial growth on different metallic surfaces.[5–8] Among these methods, the preparation of graphene through the CVD process becomes most promising because it can produce large-area single-layer graphene and, moreover, can be transferred to arbitrary substrates to fabricate graphene-based electronic devices.[6,8] Specially, graphene transferred onto an SiO_2 substrate has been the common system used for the majority of transport experiments, as it has shown the most interesting electrical transport properties.[1,6,9–11] Therefore, detailed understanding of the electronic structure for both conduction and valence bands of graphene on SiO_2 is a prerequisite to better understand the transport properties of graphene and improve the performance of graphene-based electronic devices, to which much less attention has been paid so far.[10]

Soft x-ray-absorption spectroscopy (XAS), soft x-ray-emission spectroscopy (XES), and resonant inelastic x-ray scattering (RIXS) have been confirmed to be powerful techniques for investigating carbon allotropes.[12–15] Through the matrix elements coupling the core-hole wave function to the empty and filled states, respectively, XAS and XES provide site resolved and angular momentum resolved partial densities of states (PDOS) of the conduction and valence bands.[15,16] In RIXS, one studies the variation of the XES as a function of the XAS excitation energy. Viewing the two processes as one resonant scattering process, the final state consists of a hole in the valence band and an electron in the conduction band without a core hole and contains a contribution resonant with a direct transition between the two band states at the same **k** point.[17] This process may conserve crystal momentum and hence provides a way to do band-structure mapping, which has already been successfully applied to diamond,[12] graphite,[14,18,19] C_{60},[20] C_{70},[21] SiC,[16] and LiBC.[22] It is not yet clear how the core-hole excitonic localization effect known from x-ray absorption influences the RIXS process. Is the intermediate state, which contains a core hole and an electron in the conduction band, affected by the exciton localization effect, and would it thereby breaks the translational symmetry? Or, is RIXS free from such an effect because there is no core-hole in the final state?[23–25] The uniqueness of the single-layer graphene may offer an unique model system to test if similar behavior observed in broadband metals also occurs in graphene.

In the present work, XAS, XES, and RIXS measurements have been employed to study the electronic properties of graphene on an SiO_2 substrate. Furthermore, calculations of the **k**-conserving RIXS spectra of graphene have been carried out within the Kramers-Heisenberg formulation,[26–28] including the relevant matrix elements. A key point in comparing theory with experiment for such spectra is the alignment between the XAS and XES with empty and filled PDOS, respectively. We show that the presence or absence of the core hole in the final state of these two processes, respectively, requires a shift in the alignment.

II. EXPERIMENTAL AND COMPUTATIONAL METHODS

The experiments were performed on the undulator beamline 7.0.1[20] at Advanced Light Source, Lawrence Berkeley National Laboratory. The XAS measurements were performed in total-electron-yield mode from a sample drain current with the resolution at 0.1 eV. The emission spectra were measured with a grazing incident grating spectrometer mounted with its

optical axis perpendicular to the incident x-ray beam and in the direction of the polarization vector. The resolution of both the monochromator and spectrometer were set to 0.45 eV for the XES and RIXS measurements. All the emission spectra were acquired in the same time scale and normalized to unity for the strongest inelastic emission feature in each spectrum. Single-layer graphene on an SiO_2 substrate was prepared following the method described in Ref. 6. The microstructure and quality of the graphene films were characterized by Raman spectroscopy (ISA Groupe Horiba) using a 488-nm-wavelength laser.

The band structure of graphene was calculated using the full-potential linearized muffin-tin orbital (FP-LMTO) method[29] in the local-density approximation.[30] The **k**-conserving parts or coherent RIXS spectra were calculated in the Kramers-Heisenberg formalism as described in Ref. 31.

III. RESULTS AND DISCUSSIONS

The XAS measurement recorded across the C *K* edge of graphene on an SiO_2 substrate is shown in Fig. 1(a). Figure 1(b) shows the C *K*-edge RIXS spectra with the variation of the excitation energy above the absorption threshold. These emission spectra were detected at 30° from the surface normal, and the excitation energy separation between the successive spectra was not uniform. For comparison, the uppermost XES spectrum with the excitation energy at 320.0 eV is also shown.

For the RIXS spectra, the strong emission peak located at high emission energy denotes the elastic scattering channel and

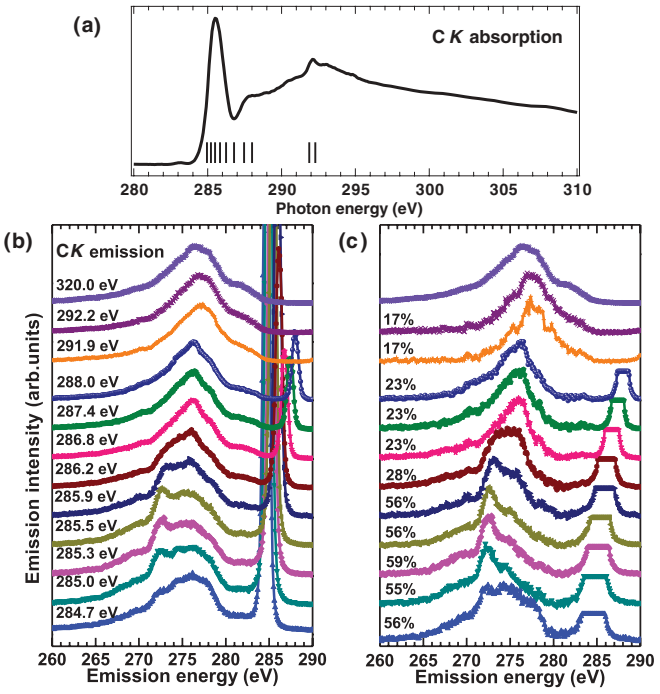

FIG. 1. (Color online) (a) C *K*-edge XAS spectrum of single-layer graphene on SiO_2. The bars indicate where RIXS spectra have been recorded. (b) XES and RIXS spectra recorded with different excitation energies as indicated in the figure. (c) Coherent fraction of the RIXS spectra in (b). The percentage values indicate the coherent contributions to the measured spectra. All the emission spectra have been normalized by the strongest inelastic peak in each spectrum.

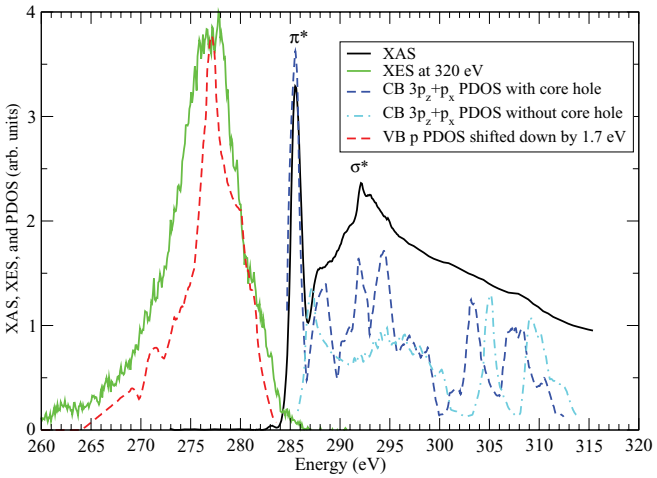

FIG. 2. (Color online) XAS and XES spectra compared to theory; see text for details.

shifts to higher emission energies as a function of the excitation energy. The spectral shape of the inelastic features presents a strong dependence on the excitation energy. However, the **k**-conserving resonant contribution is only part of this spectrum[12,18] and contributes less for the spectra at higher excitation energies.[16,28] The incoherent fraction can be viewed as representing the nonresonant XES contribution.[12,18] This contribution is maximally subtracted under the condition that the spectrum should nowhere become negative and leads to the indicated fractions of the coherent part of the spectrum shown in Fig. 1(c). In this figure, the elastic peaks are topped off for clarity.

Figure 2 shows a comparison of the XAS and XES spectra with various theoretical models. According to the widely accepted final-state rule, the XAS spectrum should reflect the PDOS in the presence of the core hole. We therefore carried out calculations in a $2 \times 2 \times 1$ supercell with a core hole included on the central atom, which means that its three nearest neighbors as well as the six next-nearest neighbors do not have a core hole. The presence of a core hole significantly changes the local density of states (DOS) compared to the unperturbed graphene and pulls a bound state out of the conduction band. This is illustrated in Fig. 3, which shows the PDOS on the core-hole atom and the nearest- and second-nearest-neighbor

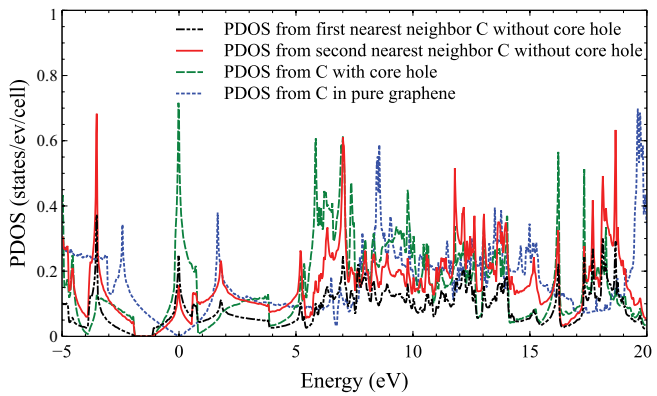

FIG. 3. (Color online) Carbon *p*-like PDOS in graphene: core-hole effect.

atoms, compared with that on a carbon atom in a primitive unit cell without a core hole. We can clearly see that a bound state is pulled out of the conduction band, and even on the second-nearest-neighbor atoms the PDOS still has significant weight on the bound state. This indicates that the core hole affects not only the atom on which the core hole is located but also its nearest neighbors. A shift of about 1.7 eV can be seen between the core-hole bound state and the π^* peak in the undisturbed graphene.

Because the incident x-ray beam is at 60° from normal and is *s* polarized, the XAS spectrum can be modeled by a $\frac{3}{4}p_z + \frac{1}{4}p_x$ PDOS. This conduction-band PDOS on the atom including the core hole is shown by the blue dashed line in Fig. 2, with the bound-state peak (or core exciton) aligned with the experimental π^* peak. The corresponding weighted PDOS from a carbon without the core hole in perfect-crystal graphene is shown as the dash-dotted cyan line. We can see that the theory including the core-hole effect much better accounts for the experimental line shape, especially for the shape of the onset beyond the bound state up to about 290.0 eV and the location of the σ^* peak relative to the π^* peak. Even peaks up to about 310.0 eV can be recognized as weak features in the experiment.

Returning now to the XES in Fig. 2, it should be represented by the PDOS without a core hole according to the final-state rule. Furthermore, because in the XES process no polarization sensing is done, we compare directly with the total *p*-like PDOS without relative weighting of the p_z and p_x in pure graphene. We find that in order to align this with the XES spectrum we need to shift down the calculated spectrum by about 1.7 eV (see Fig. 2). This can be explained by the fact that the core hole, which pulled down the PDOS by about 1.7 eV, is not present in the final state of XES, and hence the experimental spectrum should be shifted up by 1.7 eV to undo this core-hole shift. Because we know precisely where the Dirac point in the band structure occurs relative to the π^* peak of the PDOS without a core hole, and this is in fact very close to the position of the π^* bound state with a core hole, we can identify the Dirac point as occurring at 284.7 eV in the XAS spectrum.

To understand the **k**-dependent RIXS spectra in more detail, we have simulated the RIXS spectra for graphene based on the Kramers-Heisenberg equation[12,14,28] given by Eq. (1):

$$\left[\frac{d\sigma}{d\Omega d\omega_2}\right]_{\alpha\beta} \propto \sum_k \sum_{cv} \left| \frac{\langle ck|p_\alpha|s\rangle\langle s|p_\beta|vk\rangle}{E_{ck} - E_s - \omega_1 - i\Gamma/2} \right|^2 \times \delta(\omega_1 - \omega_2 - E_{ck} + E_{vk}). \quad (1)$$

Here, $\langle ck|$ and $|vk\rangle$ represent the conduction-band and valence-band states at **k**, with energies E_{ck}, E_{vk}; $|s\rangle$ is the core-hole state with energy E_s; p_α and p_β denote the momentum operators for the incoming and outgoing beam polarization, with energies ω_1 and ω_2, respectively. Γ is the core-hole lifetime.

In the calculations, we consider XAS and XES energies relative to the Dirac point. According to the alignments worked out above from the XAS and XES with PDOS, the spectrum at XAS energy ω_1 at 284.7 eV should correspond to excitation at the Dirac point, but the calculated spectrum should then be shifted up by 283.0 eV as was done with the nonresonant XES because the core hole does not affect the position of the RIXS spectrum; if it did, then the periodicity and hence the

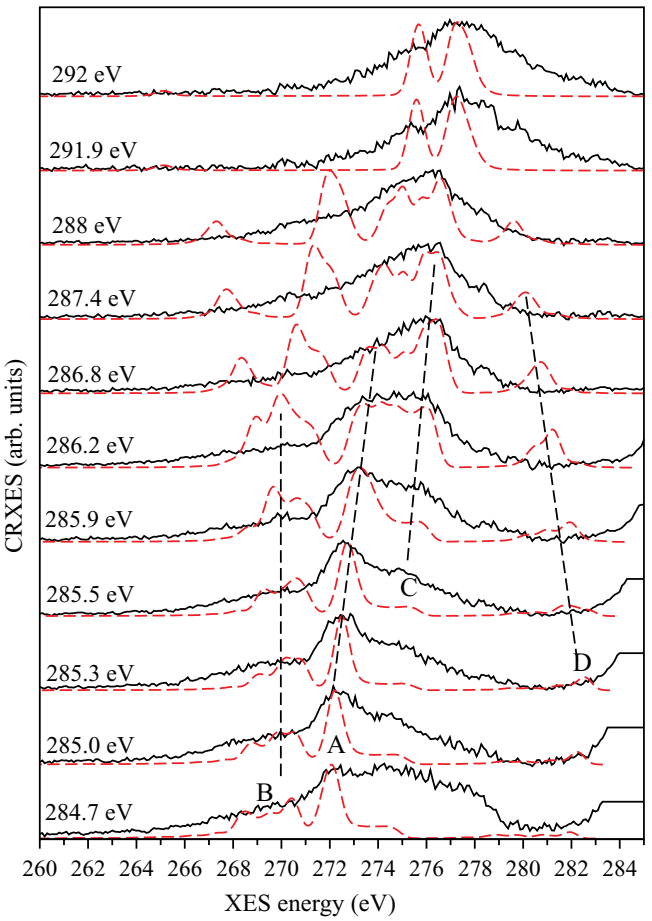

FIG. 4. (Color online) RIXS spectra (black lines) compared with calculated spectra (red lines) at different excitation energies. Both the experimental and calculated RIXS spectra have been normalized by the strongest inelastic peak in each spectrum.

k conservation would be broken. The calculated spectra for various excitation energies are shown and compared with the experimental spectra with this alignment in Fig. 4. In other words, the above analysis allows us to determine which theory spectrum to align with which experimental spectrum and how to align their energy axes. The experimental spectra shown here are more precisely the RIXS in which the incoherent fraction was removed according to the procedure mentioned earlier.

Various features in the RIXS spectra are labeled with letters in Fig. 4 for the ease of the following discussion. The dashed lines are guides for the eye on how these features disperse with excitation energies. Figure 5 shows the band structure and DOS in pure graphene and indicates the feature correlation with the bands, or band mapping. First, we note that at low excitation energies we essentially see emission from the σ bands only. This is because the emitted beam is at right angles from the incoming beam, i.e., 30° from normal, and hence primarily corresponds to in-plane polarization. The low excitation energies are close to the Dirac point or K point in the Brillouin zone (BZ). There is very little DOS at this point, and hence the spectral weight is low. It is worth mentioning that Fig. 4 shows calculated spectra scaled by peak height but the absolute intensity is weak for the low excitation energies. So, the feature labeled A corresponds to the σ band close to

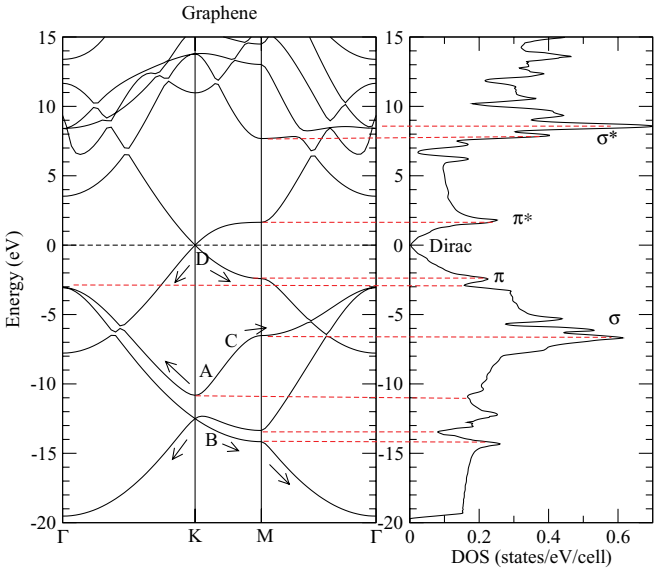

FIG. 5. (Color online) Band structure and DOS of graphene.

K. The fact that feature B below it extends down to several eV indicates that we pick up contributions from some range of **k** points near K in the spectrum. This is related to the core-hole lifetime broadening factor Γ in Eq. (1).

The fine structure of this peak is not resolved in the experiment, but the broad shoulder extending down to 265.0 eV is clearly visible in all the experimental spectra. As we increase the excitation energy, it can be seen that these features shift because we move away from K toward Γ and M. The lower band (feature B) moves down, and the upper one (feature A) moves up. At about 285.5-eV excitation energy, a new feature, C, appears, which disperses upward and grows in intensity. This is because we approach the M point in the BZ. At M, there is a large density of states due to a saddle point in the band structure (see Fig. 5). The agreement between theory and experiment in terms of the shape of the spectrum is particularly good in the range 285.0–288.0 eV.

Feature D in the theory corresponding to the π^*-π emission at M is not visible in the experiment. This could be because the emission by π bands is symmetry forbidden because the π and π^* states of the two carbon atoms in the graphene unit cell have opposite phase relations.[14,32] However, a weak π^*-π emission feature has been observed for graphite, which was attributed to the inequivalence of carbon sites in the presence of A-B-A-B stacking.[14] Our calculations show that feature D gradually increases in intensity as we move from K toward M, where the π and π^* peaks occur in the DOS. The reason why this weak feature is not seen may also in part be due to the fact that it occurs in an energy range close to the large elastic peak, and therefore the subtractions of the incoherent part and elastic peak may have removed the feature all together. In other words, it is hidden under the tail of the elastic peak. At higher excitation energies, the relation with the **k** points becomes less clear because then the excitation energies intersect the conduction bands at various points, including near Γ. The dispersion of the A, B, and C features is similar to that observed for graphite by Carlisle *et al.*[14] and shows the similarity of the overall band structure of graphite and graphene. The experimental spectra for 284.7–285.5 eV as excitation energies show considerable spectral weight in the range 274.0–280.0 eV, which is not accounted for in the calculated RIXS spectra. This may be because of imperfect subtraction of the incoherent part or may indicate sources of carbon different from pure graphene, such as defective states due to the interaction with the substrate,[32] which could be expected to affect π-bonded states in this energy range.

While the Krames-Heisenberg simulations confirm the major features to be related to the band dispersion in graphene in a similar manner as in graphite,[14] their explicit calculation provides further insight into the evolution of the spectral shape of the RIXS with variation of the XAS excitation energy, as discussed regarding the evolution of the calculated features above. The band mapping assumption that at each XAS energy the bands only intersect at a few **k** points and then the bands in XES are calculated from just those **k** points is somewhat oversimplified.[16] The core-hole electron interaction and matrix elements were previously included in the study of RIXS spectra for graphite by Carlisle *et al.*,[33] using the Bethe-Salpeter equation.[34] Our present approach has the advantage that it can be more readily included in a band-structure code and defers the core-hole interaction effects to the questions of alignment discussed earlier in this paper. This provides a simpler perspective on these effects.

IV. CONCLUSIONS

To conclude, the electronic properties and band dispersion of graphene on SiO_2 have been investigated by XAS, XES, and RIXS and analyzed using first-principles calculations. The RIXS spectra show distinct dispersive features and are interpreted as being due to the conservation of crystal momentum during the RIXS process. Kramers-Heisenberg calculations of the **k**-conserving RIXS spectra display the same band dispersion trends as in graphite. However, in order to obtain an optimal agreement between the simulated and experimental RIXS spectral shapes with varying XAS excitation energies, the shift between XAS and XES energy scales due to the presence or absence of the core hole in the final state of these two processes, respectively, has to be taken into account. This shift was shown to be consistent with the observed changes in calculated PDOS induced by the presence of the core hole.

ACKNOWLEDGMENTS

L.Z. and J.F.Z. gratefully acknowledge financial support from the National NSF of China (Grant No. 21173200), the Specialized Research Fund for the Doctoral Program of Higher Education of the Ministry of Education (Grant No. 20113402110029), and the National Basic Research Program of China (Grant No. 2010CB923302). N.S. and S.L. thank the Thailand Research Fund for an Royal Golden Jubilee scholarship (Grant No. PHD/0089/2551). The work at Case Western Reserve University was supported by NSF Grant No. DMR-1104595. The Advanced Light Source is supported by the US Department of Energy under Contract No. DE-AC02-05CH11231.

*jfzhu@ustc.edu.cn
†walter.lambrecht@case.edu
‡jguo@lbl.gov

[1] K. S. Novoselov, A. K. Geim, S. V. Morozov, D. Jiang, Y. Zhang, S. V. Dubonos, I. V. Grigorieva, and A. A. Firsov, Science **306**, 666 (2004).
[2] C. Lee, X. D. Wei, J. W. Kysar, and J. Hone, Science **321**, 385 (2008).
[3] M. Y. Han, B. Ozyilmaz, Y. B. Zhang, and P. Kim, Phys. Rev. Lett. **98**, 206805 (2007).
[4] C. Berger, Z. M. Song, X. B. Li, X. S. Wu, N. Brown, C. Naud, D. Mayou, T. B. Li, J. Hass, A. N. Marchenkov, E. H. Conrad, P. N. First, and W. A. de Heer, Science **312**, 1191 (2006).
[5] Y. S. Dedkov, M. Fonin, U. Rüdiger, and C. Laubschat, Phys. Rev. Lett. **100**, 107602 (2008).
[6] X. S. Li, W. W. Cai, J. H. An, S. Kim, J. Nah, D. X. Yang, R. Piner, A. Velamakanni, I. Jung, E. Tutuc, S. K. Banerjee, L. Colombo, and R. S. Ruoff, Science **324**, 1312 (2009).
[7] A. Reina, X. T. Jia, J. Ho, D. Nezich, H. B. Son, V. Bulovic, M. S. Dresselhaus, and J. Kong, Nano Lett. **9**, 30 (2009).
[8] W. H. Lee, J. Park, S. H. Sim, S. Lim, K. S. Kim, B. H. Hong, and K. Cho, J. Am. Chem. Soc. **133**, 4447 (2011).
[9] H. L. Cao, Q. K. Yu, L. A. Jauregui, J. Tian, W. Wu, Z. Liu, R. Jalilian, D. K. Benjamin, Z. Jiang, J. Bao, S. S. Pei, and Y. P. Chen, Appl. Phys. Lett. **96**, 122106 (2010).
[10] K. R. Knox, S. Wang, A. Morgante, D. Cvetko, A. Locatelli, T. O. Mentes, M. A. Nino, P. Kim, and R. M. Osgood, Phys. Rev. B **78**, 201408 (2008).
[11] Y. Lee, S. Bae, H. Jang, S. Jang, S.-E. Zhu, S. H. Sim, Y. I. Song, B. H. Hong, and J.-H. Ahn, Nano Lett. **10**, 490 (2010).
[12] Y. Ma, N. Wassdahl, P. Skytt, J. Guo, J. Nordgren, P. D. Johnson, J. E. Rubensson, T. Boske, W. Eberhardt, and S. D. Kevan, Phys. Rev. Lett. **69**, 2598 (1992).
[13] Y. Ma, P. Skytt, N. Wassdahl, P. Glans, D. C. Mancini, J. Guo, and J. Nordgren, Phys. Rev. Lett. **71**, 3725 (1993).
[14] J. A. Carlisle, E. L. Shirley, E. A. Hudson, L. J. Terminello, T. A. Callcott, J. J. Jia, D. L. Ederer, R. C. C. Perera, and F. J. Himpsel, Phys. Rev. Lett. **74**, 1234 (1995).
[15] J. H. Guo and J. Nordgren, J. Electron Spectrosc. Relat. Phenom. **110**, 105 (2000).
[16] J. Lüning, J. E. Rubensson, C. Ellmers, S. Eisebitt, and W. Eberhardt, Phys. Rev. B **56**, 13147 (1997).
[17] A. Kotani and S. Shin, Rev. Mod. Phys. **7**, 203 (2001).
[18] P. Skytt, P. Glans, D. C. Mancini, J. H. Guo, N. Wassdahl, J. Nordgren, and Y. Ma, Phys. Rev. B **50**, 10457 (1994).
[19] A. V. Sokolov, E. Z. Kurmaev, S. Leitch, A. Moewes, J. Kortus, L. D. Finkelstein, N. A. Skorikov, C. Xiao, and A. Hirose, J. Phys.: Condens. Matter **15**, 2081 (2003).
[20] J. H. Guo, P. Glans, P. Skytt, N. Wassdahl, J. Nordgren, Y. Luo, H. Ågren, Y. Ma, T. Warwick, P. Heimann, E. Rotenberg, and J. D. Denlinger, Phys. Rev. B **52**, 10681 (1995).
[21] J. H. Guo, P. Skytt, N. Wassdahl, J. Nordgren, Y. Luo, O. Vahtras, and H. Ågren, Chem. Phys. Lett. **235**, 152 (1995).
[22] P. F. Karimov, N. A. Skorikov, E. Z. Kurmaev, L. D. Finkelstein, S. Leitch, J. MacNaughton, A. Moewes, and T. Mori, J. Phys.: Condens. Matter **16**, 5137 (2004).
[23] P. A. Brühwiler, A. J. Maxwell, C. Puglia, A. Nilsson, S. Andersson, and N. Mårtensson, Phys. Rev. Lett. **74**, 614 (1995).
[24] P. A. Brühwiler, P. Kuiper, O. Eriksson, R. Ahuja, and S. Svensson, Phys. Rev. Lett. **76**, 1761 (1996).
[25] J. A. Carlisle, E. L. Shirley, E. A. Hudson, L. J. Terminello, T. A. Callcott, J. J. Jia, D. L. Ederer, R. C. C. Perera, and F. J. Himpsel, Phys. Rev. Lett. **76**, 1762 (1996).
[26] E. L. Shirley, J. Electron Spectrosc. Relat. Phenom. **110**, 305 (2000).
[27] J. A. Carlisle, S. R. Blankenship, L. J. Terminello, J. J. Jia, T. A. Callcott, D. L. Ederer, R. C. C. Perera, and F. J. Himpsel, J. Electron Spectrosc. Relat. Phenom. **110**, 323 (2000).
[28] S. Eisebitt and W. Eberhardt, J. Electron Spectrosc. Relat. Phenom. **110**, 335 (2000).
[29] M. Methfessel, M. Van Schilfgaarde, and R. A. Casali, *Electronic Structure and Physical Properties of Solids: The Use of the LMTO Method* (Springer-Verlag, Berlin, 2000), pp. 1–458.
[30] U. Von Barth and L. Hedin, J. Phys. C **5**, 2064 (1972).
[31] A. R. H. Preston, A. DeMasi, L. F. J. Piper, K. E. Smith, W. R. L. Lambrecht, A. Boonchun, T. Cheiwchanchamnangij, J. Arnemann, M. van Schilfgaarde, and B. J. Ruck, Phys. Rev. B **83**, 205106 (2011).
[32] S. Rajasekaran, S. Kaya, T. Anniyev, H. Ogasawara, and A. Nilsson, Phys. Rev. B **85**, 045419 (2012).
[33] J. A. Carlisle, E. L. Shirley, L. J. Terminello, J. J. Jia, T. A. Callcott, D. L. Ederer, R. C. C. Perera, and F. J. Himpsel, Phys. Rev. B **59**, 7433 (1999).
[34] E. L. Shirley, Phys. Rev. Lett. **80**, 794 (1998).